Ab initio study of the anharmonic lattice dynamics of iron at the γ-δ phase transition

Chao-Sheng Lian, Jian-Tao Wang, and Changfeng Chen

Phys. Rev. B **92**, 184110 — Published 24 November 2015

DOI: 10.1103/PhysRevB.92.184110

Ab initio study of the anharmonic lattice dynamics of iron at the γ-δ phase transition

Chao-Sheng Lian,[1] Jian-Tao Wang,[1,*] and Changfeng Chen[2]

[1]*Beijing National Laboratory for Condensed Matter Physics, Institute of Physics, Chinese Academy of Sciences, Beijing 100190, China*
[2]*Department of Physics and High Pressure Science and Engineering Center, University of Nevada, Las Vegas, Nevada 89154, USA*

(Dated: October 30, 2015)

We report calculations of phonon dispersions of iron (Fe) at its $\gamma-\delta$ phase transition using a self-consistent *ab initio* lattice dynamical method in conjunction with an effective magnetic force approach via the antiferromagnetic approximation. Our results show that anharmonic phonon-phonon interactions play a crucial role in stabilizing the δ-Fe phase in the open bcc lattice. In contrast, the lattice dynamics of the close-packed fcc γ-Fe phase are dominated by magnetic interactions. Simultaneous considerations of the lattice anharmonic and magnetic interactions produced temperature-dependent phonon dispersions for δ-Fe and γ-Fe phases in excellent agreement with recent experimental measurements. The present results highlight the key role of lattice anharmonicity in determining the structural stability of iron at high temperatures, which has significant implications for other high-temperature paramagnetic metals like Ce and Pu.

PACS numbers: 63.20.dk, 63.20.kg, 63.70.+h, 75.50.Bb

I. Introduction

Elemental iron (Fe) exhibits fascinating structural, mechanical and magnetic properties, which have attracted great interest in many fields of science and technology. There have been extensive studies on the mechanisms underlying these properties, but the complex pressure-temperature (P-T) phase diagram of iron has presented formidable challenges to a full understanding of this important and enigmatic material. Of particular interest are the temperature-driven structural phase transitions of iron. At low temperatures, iron adopts a body-centered cubic (bcc) crystal lattice in its α phase, which is ferromagnetic below the Curie temperature $T_C = 1043$ K; two paramagnetic structural phase transitions occur as temperature increases, i.e., the transition to the face-centered cubic (fcc) γ-Fe at 1185 K and the transition to the high-temperature bcc δ-Fe at 1667 K, which is stable up to the melting temperature of 1811 K[1]. While the ground-state behavior of α-Fe is well understood within the Stoner theory of ferromagnetism[2,3], the mechanisms for the transitions to the high-temperature γ and δ phases remain unresolved. Early theoretical accounts for the phase transitions in iron were highly controversial, where pure magnetic[4,5] or vibrational[6,7] contributions to the free energy were considered to be the main driving forces. In particular, within the spin-fluctuation theory, Hasegawa *et al.*[5] ascribed the δ phase stability to the magnetic disorder in the bcc lattice at high temperatures, while Osetsky *et al.*[7] suggested by molecular dynamics simulations an alternative explanation based largely on the contributions from the vibrational entropy. It has been shown, however, that a full understanding of the phase diagram of iron requires simultaneous considerations of different contributions to the entropy in the vicinity of the transition temperatures[8].

Recent years have seen significant progress in probing thermodynamic properties of iron[9–16]. Neuhaus *et al.*[11,12] performed inelastic neutron scattering measurements of the phonon dispersions of iron at high temperatures near the distinct phase transitions, and they found that the vibrational and electronic entropies contribute almost equally at the α-γ transition, while the vibrational contribution dominates at the γ-δ transition, stemming from the low-energy transverse phonons in the open bcc lattice of the δ phase. These experimental results have provided important insights into the stability mechanisms of the high-temperature iron phases. Nevertheless, the physical interactions governing the observed unusual thermodynamics are still poorly understood, and the explanation for the unusual phonon behavior in paramagnetic iron at high temperatures still poses a great theoretical challenge.

Several computational schemes[17–23] have attempted to account for the lattice dynamics of paramagnetic iron, including a spin-space averaging (SSA) procedure[17], the dynamical mean-field theory (DMFT)[20] and a spin-spiral method[21]. By considering the finite-temperature magnetism in force-constant calculations and using the quasi-harmonic approximation (QHA) that treats only the effect of thermal lattice expansion, these approaches can reproduce the observed phonon dispersions of α-Fe and γ-Fe and generally reveal a strong effect of the magnetic short-range order on the dynamical stability of α-Fe above T_C[18–21]. Very recently, Leonov *et al.*[24] extended DMFT calculations to the high-temperature δ-Fe and found within QHA an instability of the bcc lattice, suggesting the necessity of including other anharmonic effects for a correct description of δ-Fe. Anharmonicity in the lattice subsystem, i.e., the phonon-phonon interactions[25], is especially important close to the melting point, as was seen in the bcc phases of the group 3 (Sc, Y, La) and 4 (Ti, Zr, Hf) metals[26–29]. Whether the anharmonic lattice effect is crucial in the case of iron

remains to be demonstrated. Moreover, the interplay between effects of the magnetism and the lattice anharmonicity is also unclear in high-temperature paramagnetic iron.

In this paper, using the self-consistent *ab initio* lattice dynamical (SCAILD) calculations[27,28], we explicitly incorporate the phonon-phonon interactions to determine the anharmonic phonon dispersions of both the fcc and bcc iron phases at the high-temperature γ-δ transition. We consider the effect of magnetic interactions by including the local moments in the force calculations required for SCAILD. In the high-temperature δ-Fe phase, significant phonon renormalization is found due to the phonon-phonon interactions, resulting in the dynamical stability of the open bcc lattice; whereas in the close-packed fcc γ-Fe phase, only small anharmonic lattice effects are predicted, and the magnetic interactions play a more prominent role. For both δ-Fe and γ-Fe, with simultaneous considerations of the lattice anharmonic and magnetic interactions, our calculated temperature-dependent lattice dynamical properties agree well with the experimental data.

II. Computational Details

We have performed finite-temperature phonon calculations using the SCAILD method with the Hellmann-Feynman forces obtained from *ab initio* calculations based on the density functional theory (DFT) as implemented in the VASP package[30]. The projector augmented wave (PAW) scheme[31] was used to describe the electron-ion interactions, and the generalized gradient approximation (GGA) with the Perdew-Burke-Ernzerhof parametrization[32] for the exchange-correlation functional was adopted. After running convergence tests, we have chosen the plane wave cutoff energy of 345 eV. The supercell used was obtained by increasing the bcc or fcc primitive cell 4 times along the 3 primitive lattice vectors, and all the reported calculations were performed using a uniform $4\times4\times4$ Monkhorst-Pack[33] k-point grid with a Methfessel-Paxton smearing of 0.2 eV. Thermal expansion effects were taken into account to determine the lattice constants at finite temperatures[34].

As an extension of the frozen phonon method[35], SCAILD determines phonon frequencies using the Hellmann-Feynman forces in a supercell where atoms are displaced from their equilibrium positions according to the phonon amplitudes[27,28]

$$\mathcal{A}_{\mathbf{q}s} \;=\; \pm\sqrt{\frac{\hbar}{M\omega_{\mathbf{q}s}}\left[\frac{1}{2}+n\left(\frac{\hbar\omega_{\mathbf{q}s}}{k_BT}\right)\right]}, \qquad (1)$$

where $n(x)=1/(e^x-1)$ is the Planck function, T is the absolute temperature of the system, and M is the atomic mass. Since all phonons with wave vectors $\mathbf{q}$ commensurate with the supercell contribute to the atomic displacements present in the same force calculation, the interactions between different lattice vibrations are included in the calculated phonon frequencies given by[27,28]

$$\omega_{\mathbf{q}s} \;=\; \left[-\frac{1}{M}\frac{\epsilon_{\mathbf{q}s}\cdot\mathbf{F}_{\mathbf{q}}}{\mathcal{A}_{\mathbf{q}s}}\right]^{1/2}, \qquad (2)$$

where $\mathbf{F}_{\mathbf{q}}$ is the Fourier transform of the atomic forces and $\epsilon_{\mathbf{q}s}$ is the eigenvector of phonon mode s. In view of the mutual dependence among the forces, displacements, and the phonons dictated by Eqs. (1) and (2), this approach requires a self-consistency loop to determine the temperature-dependent lattice dynamics [if imaginary phonon frequencies occur in the first iterations, the absolute values $|\omega_{\mathbf{q}s}|$ are used in Eq. (1)]. As a result, one gets from SCAILD a set of phonon frequencies that have been renormalized by anharmonic phonon-phonon interactions to all orders.

A complete description of the lattice dynamics of paramagnetic (PM) iron requires that the magnetic effect is also accounted for in addition to the anharmonic lattice effect. Because accurate force calculations in the PM state are limited in the presently available DFT implementations, we employ an antiferromagnetic (AFM) state approximation in consideration of its features shared with the PM state, specifically the local moments on the Fe atoms and the zero total magnetic moment in a unit cell. The single-layered AFM configurations along the [001] and [111] directions, being commensurate with the supercells used in the SCAILD calculations, are adopted for the bcc and fcc iron, respectively. Within these AFM approximations, phonon frequency calculations converge in about 50 iterations for the bcc phase and 30 iterations for the fcc phase. Discussion of the phonon dispersion's dependence on the AFM configuration is provided in the Supplemental Material[36].

It is crucial to note that considering an individual magnetic configuration will destroy the symmetry of a bcc or fcc crystal. To retain the correct symmetry of the calculated phonon dispersions, the symmetries of the different $\mathbf{q}$-vectors are restored for each iteration by[27,28]

$$\bar{\omega}^2_{\mathbf{q}s} \;=\; \frac{1}{m_{\mathbf{q}}}\sum_{\mathcal{S}\in\mathcal{S}(\mathbf{q})}\omega^2_{\mathcal{S}^{-1}\mathbf{q}s}, \qquad (3)$$

where $\mathcal{S}(\mathbf{q})$ is the symmetry group of the wave vector $\mathbf{q}$ and $m_{\mathbf{q}}$ is the number of elements of the group. This procedure in SCAILD is in principle equivalent to that in SSA[17] where the force constant matrix derived from a single magnetic configuration is symmetrized by employing all the lattice symmetry operations.

III. Results and discussions

We examine the lattice dynamical properties of paramagnetic iron near the γ-δ phase transition using the SCAILD method in the context of both the nonmagnetic (NM) and AFM approximations. Our results for

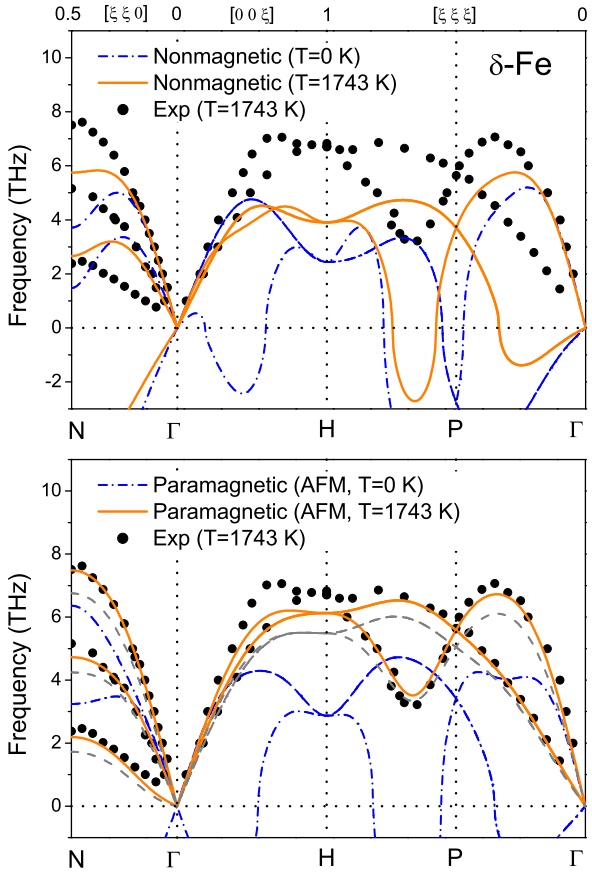

FIG. 1: (Color online) Phonon dispersions of paramagnetic δ-Fe calculated within the nonmagnetic (top) and antiferromagnetic (bottom) approximations, compared to experimental data measured at 1743 K (Ref. 12). The solid orange lines represent the self-consistent phonon calculations. The antiferromagnetic 1743 K results obtained at the experimental lattice constant (gray dashed lines) are also shown.

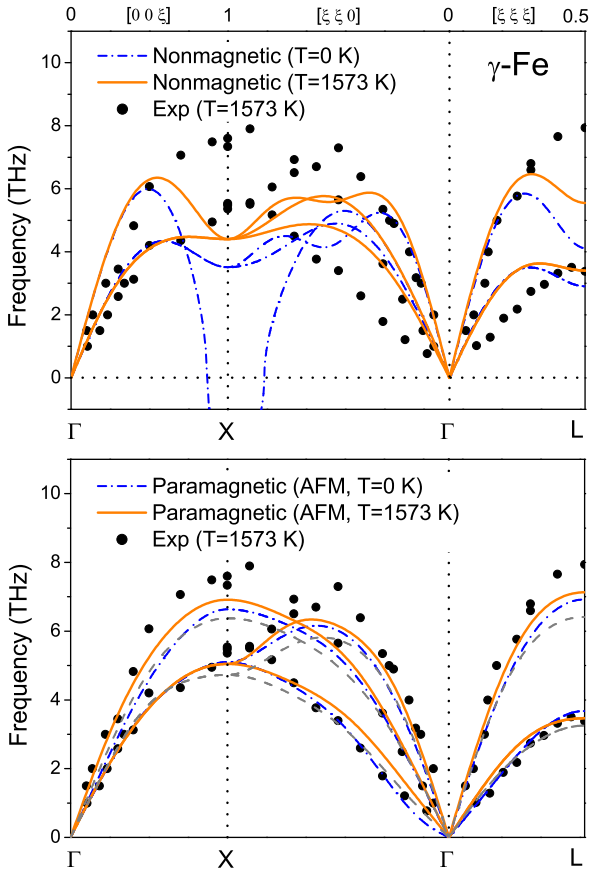

FIG. 2: (Color online) Phonon dispersions of paramagnetic γ-Fe calculated within the nonmagnetic (top) and antiferromagnetic (bottom) approximations, compared to experimental data measured at 1573 K (Ref. 12). The solid orange lines represent the self-consistent phonon calculations. The antiferromagnetic 1573 K results obtained at the experimental lattice constant (gray dashed lines) are also shown.

the phonon dispersions of δ-Fe are presented in Fig. 1. The theoretical calculations are carried out at the lattice constant a = 2.897 Å obtained for PM bcc Fe at T = 1743 K, which is only 1.1% smaller than the experimental value of 2.931 Å[1]. The NM phonon dispersions at T = 0 K (Fig. 1, top panel) show imaginary frequencies along [$\xi\xi$0], [00ξ], and [$\xi\xi\xi$], which is in agreement with the previously reported results calculated using the ultrasoft pseudopotentials[20,37]. At T = 1743 K, the SCAILD calculations predict that the bcc lattice of δ-Fe is still dynamically unstable, although the imaginary phonon frequencies along the [00ξ] direction have been removed. Under the AFM approximation, where the local magnetic moment $\mu = 1.95\ \mu_B$, the calculated phonon dispersions at T = 0 K (Fig. 1, bottom panel) also exhibit imaginary modes in the [$\xi\xi$0], [00ξ], and [$\xi\xi\xi$] directions. In sharp contrast, our finite-temperature AFM SCAILD calculations reveal a significant phonon renormalization due to the phonon-phonon interactions, which produces a strong phonon frequency hardening that removes all the imaginary phonon modes, thus successfully predicting the dynamical stability of the bcc lattice of δ-Fe at high temperatures. Furthermore, the calculated T = 1743 K phonon dispersions are in excellent agreement with recent experimental data for δ-Fe[12]. These results clearly suggest that the anharmonic phonon-phonon interactions play a key role in stabilizing the bcc δ-Fe phase at high temperatures. Note that by considering this anharmonic effect Luo *et al.*[38] had found a lattice stability P-T range of bcc Fe at the Earth's core conditions. The reported phonon dispersions for the δ phase at zero pressure therein are different from ours in terms of the highest phonon frequency at the N point (larger in the former), which can possibly be attributed to the use of a smaller lattice constant or other different parameters involved in the AFM SCAILD calculations.

We next investigate the phonon dispersions of γ-Fe, and the results are presented in Fig. 2. The theoretical calculations are performed at the lattice constant a = 3.608 Å obtained for PM fcc Fe at T = 1573 K, which is

TABLE I: The three cubic elastic constants (in GPa) deduced from the calculated phonon dispersions for δ-Fe and γ-Fe, compared to available experimental data. We also list the theoretical and experimental lattice constants.

Method	Phase	T (K)	C_{11}	C_{44}	C'	a (Å)
NM SCAILD	bcc	1743	123	78	-51	2.897
AFM SCAILD	bcc	1743	129	103	4	2.897
Expt. (Refs. 1 and 12)	bcc	1743	158	86	11	2.931
NM SCAILD	fcc	1573	361	138	100	3.608
AFM SCAILD	fcc	1573	169	85	32	3.608
Expt. (Refs. 1 and 12)	fcc	1573	171	68	18	3.672

only 1.7% smaller than the experimental value of 3.672 Å[1]. The calculated NM phonon dispersions at $T = 0$ K (Fig. 2, top panel) exhibit imaginary frequencies around the X point. The finite-temperature NM SCAILD calculations remove these imaginary modes, thus predicting that the fcc lattice of γ-Fe is dynamically stable. However, the obtained $T = 1573$ K phonon dispersion curves deviate considerably from the experimental data[12], especially for the longitudinal modes near the X and L points. Considerable improvement is achieved by invoking the AFM approximation for γ-Fe where the local magnetic moment $\mu = 1.92\ \mu_B$. In sharp contrast to the NM case, the resulting $T = 0$ K phonon dispersions (Fig. 2, bottom panel) display no imaginary frequency, thus predicting the dynamical stability of the γ-Fe fcc structure; moreover, these calculated results at $T = 0$ K are already in reasonably good agreement with experimental data[12]. The AFM SCAILD calculations at $T = 1573$ K introduce additional but small improvements compared with the experimental observations. These results demonstrate that magnetic interactions have a dominant impact on the vibrational properties of γ-Fe, and given the small extent of the phonon renormalization effect arising from the phonon-phonon interactions (confirmed also by the $T = 1200$ K results in the Supplemental Material[36]), the lattice anharmonicity in the close-packed fcc γ-Fe phase plays a much less prominent role compared with its impact on the open bcc lattice of δ-Fe phase, which is similar to the cases found in hcp Ti, Zr, and Hf[27,39].

Using phonon dispersions, we calculated the elastic properties of δ-Fe and γ-Fe. We determine the cubic elastic constants C_{11}, C_{44}, and C' by utilizing the relationships[40] $\rho V^2_{001L} = C_{11}$, $\rho V^2_{001T} = C_{44}$, and $\rho V^2_{110L} = C_{11} + C_{44} - C'$, where ρ is the density and V denotes the longitudinal (L) or transverse (T) sound velocities along the $[00\xi]$ and $[\xi\xi 0]$ directions. Our calculated results are listed in Table I and compared with experimental data[12]. It is seen that the NM SCAILD calculations are unreliable, producing a negative C' for δ-Fe and considerably overestimating the elastic constants for γ-Fe; meanwhile, the AFM SCAILD calculations produce elastic constants in good agreement with experimental data for both phases.

It is worth noting that for both δ-Fe and γ-Fe the local magnetic moments included in the AFM approximation are an essential requirement for correctly explaining their phonon behavior within SCAILD since, overall, calculations within the NM approximation produce lattice dynamical properties which differ significantly from the experimental measurements. These findings highlight the interplay between the magnetism of the electrons and the lattice degrees of freedom and underscore the importance to consider both the lattice anharmonic and magnetic effects simultaneously for a good quantitative description of the high-temperature lattice dynamics in paramagnetic iron.

In addition, we also performed AFM SCAILD calculations at the experimental lattice constants 2.931 Å for δ-Fe at 1743 K and 3.672 Å for γ-Fe at 1573 K, producing phonon dispersions showing an obvious softening compared to the measured data (see gray dashed lines in the bottom panels of Figs. 1 and 2). The discrepancy is expected to be overcome by combining the SCAILD method with advanced techniques such as the DMFT, which can avoid the use of an specific AFM configuration and treat the magnetic effect more accurately. This is, however, beyond our capability at present, and should be the direction for future research.

IV. Conclusions

We have studied the anharmonic lattice dynamics of iron at its γ-δ transition using the SCAILD method in conjunction with an effective magnetic force approach via the antiferromagnetic approximation. Our results show that the anharmonic phonon-phonon interactions are largely responsible for the stability of the bcc δ-Fe while the magnetic interactions play a dominant role in stabilizing the fcc γ-Fe. Simultaneous considerations of the two effects have led to an excellent agreement between the theoretical results and the experimental data on the temperature-dependent lattice dynamical properties in δ-Fe and γ-Fe. Finally we remark that once the magnetic effect is properly treated the SCAILD method is capable of describing the anharmonic phonon-phonon effects in paramagnetic materials, and it would be interesting to apply this method to other high-temperature paramagnetic metals such as the bcc phases of Ce and Pu[41,42].

Acknowledgments

This study was supported by the National Natural Science Foundation of China (Grant No. 11274356) and the Strategic Priority Research Program of the Chinese Academy of Sciences (Grant No. XDB07000000). C.F.C. was supported in part by the U.S. Department of Energy under Cooperative Agreement DE-NA0001982. We are thankful to the crew of the Quantum Computational Center of the Institute of Physics, Chinese Academy of Sciences, for their support at the Shuguang supercomputing facilities.

* Electronic address: wjt@aphy.iphy.ac.cn

[1] Z. S. Basinski, W. Hume-Rothery, and A. L. Sutton, Proc. R. Soc. Lond. A **229**, 459 (1955).
[2] E. C. Stoner, Proc. R. Soc. Lond. A **169**, 339 (1939).
[3] G. L. Krasko and G. B. Olson, Phys. Rev. B **40**, 11536 (1989).
[4] L. Kaufman, E. V. Clougherty, and R. J. Weiss, Acta Metall. **11**, 323 (1963).
[5] H. Hasegawa and D. G. Pettifor, Phys. Rev. Lett. **50**, 130 (1983).
[6] R. J. Weiss and K. J. Tauer, Phys. Rev. **102**, 1490 (1956).
[7] Y. N. Osetsky and A. Serra, Phys. Rev. B **57**, 755 (1998).
[8] A. T. Dinsdale, Calphad **15**, 317 (1991).
[9] Q. Chen and B. Sundman, J. Phase Equilibria **22**, 631 (2001).
[10] M. H. G. Jacobs and R. Schmid-Fetzer, Phys. Chem. Miner. **37**, 721 (2010).
[11] J. Neuhaus, W. Petry, and A. Krimmel, Physica B **234-236**, 897 (1997).
[12] J. Neuhaus, M. Leitner, K. Nicolaus, W. Petry, B. Hennion, and A. Hiess, Phys. Rev. B **89**, 184302 (2014).
[13] L. Mauger, M. S. Lucas, J. A. Muñoz, S. J. Tracy, M. Kresch, Y. Xiao, P. Chow, and B. Fultz, Phys. Rev. B **90**, 064303 (2014).
[14] V. J. Minkiewicz, G. Shirane, and R. Nathans, Phys. Rev. **162**, 528 (1967).
[15] S. K. Satija, R. P. Comes, and G. Shirane, Phys. Rev. B **32**, 3309 (1985).
[16] J. Zarestky and C. Stassis, Phys. Rev. B **35**, 4500 (1987).
[17] F. Körmann, A. Dick, B. Grabowski, T. Hickel, and J. Neugebauer, Phys. Rev. B **85**, 125104 (2012).
[18] F. Körmann, B. Grabowski, B. Dutta, T. Hickel, L. Mauger, B. Fultz, and J. Neugebauer, Phys. Rev. Lett. **113**, 165503 (2014).
[19] I. Leonov, A. I. Poteryaev, V. I. Anisimov, and D. Vollhardt, Phys. Rev. Lett. **106**, 106405 (2011).
[20] I. Leonov, A. I. Poteryaev, V. I. Anisimov, and D. Vollhardt, Phys. Rev. B **85**, 020401 (2012).
[21] A. V. Ruban and V. I. Razumovskiy, Phys. Rev. B **85**, 174407 (2012).
[22] S. V. Okatov, A. R. Kuznetsov, Y. N. Gornostyrev, V. N. Urtsev, and M. I. Katsnelson, Phys. Rev. B **79**, 094111 (2009).
[23] H. Zhang, B. Johansson, and L. Vitos, Phys. Rev. B **84**, 140411 (2011).
[24] I. Leonov, A. I. Poteryaev, Y. N. Gornostyrev, A. I. Lichtenstein, M. I. Katsnelson, V. I. Anisimov, and D. Vollhardt, Sci. Rep. **4**, 5585 (2014).
[25] B. Fultz, Prog. Mater. Sci. **55**, 247 (2010).
[26] W. Petry, J. Phys. IV **05**, C2-15 (1995).
[27] P. Souvatzis, O. Eriksson, M. I. Katsnelson, and S. P. Rudin, Phys. Rev. Lett. **100**, 095901 (2008).
[28] P. Souvatzis, O. Eriksson, M. I. Katsnelson, and S. P. Rudin, Comput. Mater. Sci. **44**, 888 (2009).
[29] P. Souvatzis, T. Björkman, O. Eriksson, P. Andersson, M. I. Katsnelson, and S. P. Rudin, J. Phys. Condens. Matter **21**, 175402 (2009).
[30] G. Kresse and J. Furthmüller, Phys. Rev. B **54**, 11169 (1996).
[31] P. E. Blöchl, Phys. Rev. B **50**, 17953 (1994).
[32] J. P. Perdew, K. Burke, and M. Ernzerhof, Phys. Rev. Lett. **77**, 3865 (1996).
[33] H. J. Monkhorst and J. D. Pack, Phys. Rev. B **13**, 5188 (1976).
[34] The experimental lattice expansion coefficients[1,23] [14.5×10^{-6} (bcc) and 23.8×10^{-6} (fcc) 1/K] have been combined with the theoretical lattice constants of 2.825 Å for PM bcc Fe and 3.478 Å for PM fcc Fe at $T = 0$ K, respectively. See the Supplemental Material[36] for more details.
[35] B. N. Harmon, W. Weber, and D. R. Hamann, Phys. Rev. B **25**, 1109 (1982).
[36] See Supplemental Material at [] for the phonon dispersion's dependence on the AFM configuration, the phonon dispersions of γ-Fe at $T = 1200$ K, and the theoretical lattice constants of PM Fe.
[37] H. C. Hsueh, J. Crain, G. Y. Guo, H. Y. Chen, C. C. Lee, K. P. Chang, and H. L. Shih, Phys. Rev. B **66**, 052420 (2002).
[38] W. Luo, B. Johansson, O. Eriksson, S. Arapan, P. Souvatzis, M. I. Katsnelson, and R. Ahuja, Proc. Natl. Acad. Sci. USA **107**, 9962 (2010).
[39] P. Souvatzis, S. Arapan, O. Eriksson, and M. I. Katsnelson, Europhys. Lett. **96**, 66006 (2011).
[40] D. J. Dever, J. Appl. Phys. **43**, 3293 (1972).
[41] K. Nicolaus, J. Neuhaus, W. Petry, and J. Bossy, Eur. Phys. J. B **21**, 357 (2001).
[42] X. Dai, S. Y. Savrasov, G. Kotliar, A. Migliori, H. Ledbetter, and E. Abrahams, Science **300**, 953 (2003).